

# Giant magnetoelectric coupling and *E*-field tunability in a laminated Ni<sub>2</sub>MnGa/lead-magnesium-niobate-lead titanate multiferroic heterostructure

Yajie Chen,<sup>1,a)</sup> Jingmin Wang,<sup>2</sup> Ming Liu,<sup>1</sup> Jing Lou,<sup>1</sup> Nian X. Sun,<sup>1</sup> Carmine Vittoria,<sup>1</sup> and Vincent G. Harris<sup>1</sup>

<sup>1</sup>Center for Microwave Magnetic Materials and Integrated Circuits, and the Department of Electrical and Computer Engineering, Northeastern University, Boston, Massachusetts 02115, USA

<sup>2</sup>Department of Materials Science and Engineering, Massachusetts Institute of Technology, Cambridge, Massachusetts 02139, USA

(Received 9 August 2008; accepted 27 August 2008; published online 15 September 2008)

The multiferroic properties of a laminated heterostructure consisting of magnetostrictive Ni<sub>2</sub>MnGa ribbon and piezoelectric lead-magnesium-niobate-lead titanate crystal are reported. A tunability of the electric field-induced magnetic field was measured by a shift in the ferromagnetic resonance (FMR) field by 230 Oe at *X*-band while applying an electric field of 6 kV/cm. Concomitantly, a frequency shift in the FMR of 370 MHz was observed. The sensitive tunability stems from a large linear magnetoelectric coupling coefficient,  $A=41$  Oe cm/kV, measured in the heterostructure. This represents a new class of metallic multiferroic heterostructures that operate at microwave frequencies. © 2008 American Institute of Physics. [DOI: 10.1063/1.2986480]

Multiferroic materials have invigorated interest in the fields of ferroelectric, ferromagnetic, and multifunctional materials. Such materials, which simultaneously display ferroelectricity and ferromagnetism, can typically be realized by two materials design paths, that is, as “natural” multiferroic single phase compounds, or as “artificial” multiferroic composites or heterostructures. However, most single phase multiferroic materials exhibit a magnetoelectric response at low temperatures,<sup>1</sup> severely hindering their use in practical engineering devices. In contrast, the artificially structured materials, typically constructed as multilayered heterostructures or as granular composites, often exhibit large magnetoelectric coupling at or above room temperature.<sup>2,3</sup> Comparatively, these artificial materials offer greater potential and opportunity for exploring novel multifunctional devices, such as magnetic field sensors, transducers, filters, oscillators, phase shifters, memory devices, etc.<sup>4</sup> As a result, there has been a great amount of interest in understanding both the fundamental physics as well as the engineering potential of these materials and structures.<sup>5,6</sup>

The Ni<sub>2</sub>MnGa Heusler alloy has received considerable interest as a magnetic shape memory alloy. However, Ni<sub>2</sub>MnGa also possesses a large magnetostriction coefficient,  $\lambda_{001}=-3100$  ppm at  $H=6$  kOe, near room temperature (23–31 °C).<sup>7</sup> This property provides a unique opportunity for its incorporation in multiferroic structures where electric field-induced elastic deformation in the Heusler alloy may result in a large magnetoelectric coupling coefficient.

The present work is focused on a layered multiferroic structure consisting of a ferromagnetic magnetostrictive Ni<sub>2</sub>MnGa alloy and ferroelectric lead magnesium niobate-lead titanate (PMN-PT). Our interest is in the demonstration of magnetoelectric interactions at *X*-band (i.e.,  $f\sim 10$  GHz) microwave frequencies in this unique structure. The magnetostrictive ribbons, obtained by melt spinning an alloy ingot of the nominal composition Ni<sub>51</sub>Mn<sub>27.5</sub>Ga<sub>21.5</sub>, have thicknesses of  $\sim 40$   $\mu\text{m}$ , and show a tetragonal martensitic phase

at room temperature. It is noteworthy that the PMN-PT single crystal, with 28%–32% PT, features anisotropic in-plane piezoelectric coefficients,  $d_{31}=-1800$  pC/N and  $d_{32}=900$  pC/N, while poling along with (011).<sup>8</sup>

The multiferroic composite explored here was designed to operate in the *L-T* ME coupling mode (i.e., longitudinal magnetized/transverse polarized) and is a laminated structure consisting of Ni<sub>2</sub>MnGa ribbon and PMN-PT single crystal poled along with (011). The two components were bonded with an ethyl cyanoacrylate glue. The ferromagnetic resonance (FMR) measurements were carried out using a microwave cavity excited in a TE<sub>102</sub> mode at *X*-band ( $f=9.53$  GHz). The external field  $H_0$  is aligned parallel to the  $d_{31}$  direction of the PMN-PT crystal for magnetoelectric coupling measurements. All of the measurements were carried out at room temperature ( $\sim 23$  °C).

Figure 1(a) shows the results of static magnetic measurements for the Ni<sub>2</sub>MnGa ribbon using vibrating sample magnetometry. In the in-plane measurement, the saturation magnetization and coercivity are  $4\pi M_s=6.6$  kG and  $H_c=255$  Oe, respectively. The out-of-plane measurement shows a sheared hysteresis loop, which arises predominantly from the demagnetizing field of the ribbon. Additionally, the angular dependence of the magnetization in the plane of the ribbon remains nearly constant, which reflects in-plane isotropic magnetic properties. However, the x-ray diffraction measurements reveal a slight, but significant, preferential alignment of (110) oriented grains along the out-of-plane direction, as shown in the inset of Fig. 1(a).

Next, we measure magnetization curves while applying an electric field across the PMN-PT crystal in order to investigate the magnetoelectric coupling in a static magnetic state. In this case, an induced magnetic field is generated in response to the application of an electric field of 6 kV/cm, as depicted in Fig. 1(b). In particular, the *E*-field induced magnetic field shift can be clearly observed in a magnetic field of 4–7 kOe, corresponding to a magnetization curve shift of 120–170 Oe, as shown in the upper inset to Fig. 1(b). Although the lower inset to Fig. 1(b) illustrates the dependence

<sup>a)</sup>Electronic mail: y.chen@neu.edu.

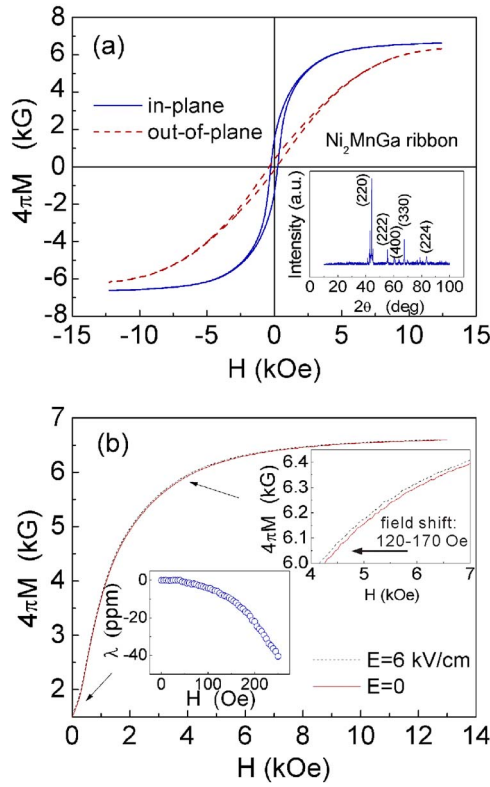


FIG. 1. (Color online) (a) Magnetic hysteresis for  $\text{Ni}_2\text{MnGa}$  ribbon having a thickness of  $40 \mu\text{m}$ . Solid line and dash line represent the in-plane and out-of-plane measurements, respectively. Inset shows x-ray diffraction  $\theta$ - $2\theta$  spectrum. (b) In-plane magnetization curves of the  $\text{Ni}_2\text{MnGa}/\text{PMN-PT}$  composite with electric field strengths of 0 and 6 kV/cm. The upper inset shows an enlarged portion of the magnetization curve, indicating the field shifts under an electric field, whereas the lower inset shows a measurement of magnetostriction constant vs magnetic field for the  $\text{Ni}_2\text{MnGa}$  ribbon.

of the magnetostriction constant,  $\lambda$ , upon magnetic field ranging from 0 to 250 Oe, the measurement occurs far from the region in the  $d\lambda/dH$  curve near the maximum.<sup>7</sup> These results unambiguously corroborate that the magnetoelectric coupling mediates the elastic deformation in the Heusler alloy ribbon and the subsequent generation of the magnetic field in this layered structure.

The solid line in Fig. 2 represents the influence of the electric field strength on the FMR spectrum. It is noteworthy

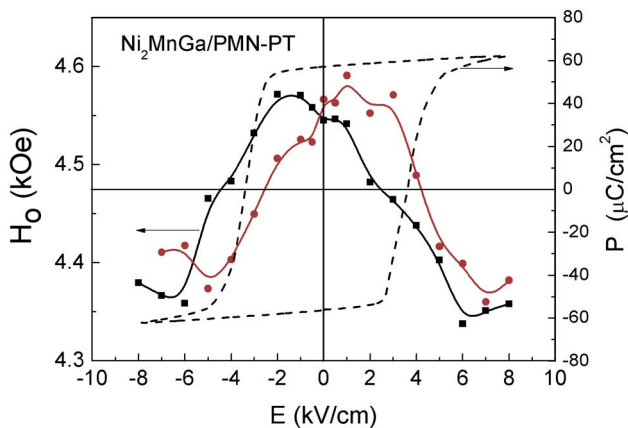


FIG. 2. (Color online) Dependence of FMR external field on the applied electric field in the laminated  $\text{Ni}_2\text{MnGa}/\text{PMN-PT}$  composite (solid line  $\rightarrow$ ), and the polarization hysteresis loop for the ferroelectric lead PMN-PT crystal used in the laminated composite (dash line  $\rightarrow$ ).

that the electric field facilitates a decrease in the resonance field, which yields a maximum shift of  $\sim 230$  Oe at  $E = 6$  kV/cm. The decrease in the external magnetic field is compensated with an increase in the stress-induced internal magnetic field. Additionally, the  $H_0$  versus  $E$  curve clearly displays the familiar butterfly shape, which is attributed to the correlation between strain and electric field. Alternatively, the irreversible strain with electric field results from the ferroelectric hysteresis phenomenon, which is also presented for the PMN-PT crystal as the dashed line in Fig. 2. Since this two-layer structure has a small magnetic filling factor, i.e., 40/500 or 0.08 as the magnetic film to PMN-PT crystal ratio, the strain-induced internal magnetic field can be simply expressed as<sup>9</sup>

$$\delta H_E = \frac{3\lambda Y d_{31} E_3}{M} = AE, \quad (1)$$

where  $A$  is the magnetoelectric constant;  $\lambda$  and  $Y$  are magnetostriction constant and Young's modulus of the  $\text{Ni}_2\text{MnGa}$  ribbon, respectively;  $d_{31}$  and  $E_3$  denote the piezoelectric coefficient and electric field across PMN-PT slab, respectively. The stress-induced magnetic field is estimated to be  $\delta H_E \approx 780$  Oe, where  $\lambda = -40$  ppm,  $Y = 2.8 \times 10^{12}$  dyn/cm<sup>2</sup>,<sup>10</sup>  $d_{31} = -1750$  pC/N,  $E_3 = 6$  kV/cm, and  $M = 477$  G. Note, that the estimated value is far greater than that measured experimentally. However, it is predicted that a theoretic estimate is even greater than  $\delta H_E \approx 780$  Oe when considering that  $\lambda$  at  $H = 4.5$  kOe is likely  $\leq -100$  ppm.<sup>7</sup> The discrepancy is mainly attributed to the effective coupling between the PMN-PT crystal and the  $\text{Ni}_2\text{MnGa}$  ribbon. For example, the stress driven by the application of an electric field is mostly transferred to the glue bonding layer having a relatively small Young's modulus. Moreover, the induced magnetic field depends sensitively upon the thickness of the glue layer. Nevertheless, a significant magnetoelectric constant,  $\sim 40$  Oe cm/kV, is measured for this MF heterostructure. This figure of merit is much larger than those previously observed in other layered structures (see Table I).<sup>4,11-13</sup>

The FMR measurements were carried out with an applied magnetic field aligned along the in-plane and out-of-plane sample directions. The FMR linewidths,  $\Delta H$ , range from 1200 to 2000 Oe at X-band, which is in agreement with previous publications.<sup>14</sup> Given no applied electric field, the two resonance conditions can be expressed as in Eqs. (2) and (3),<sup>15</sup>

$$\text{In-plane measurement: } f = \gamma \sqrt{H_0^{\parallel} (H_0^{\parallel} + 4\pi M_{\text{eff}}^{\parallel})}, \quad (2)$$

$$\text{Out-of-plane measurement: } f = \gamma \sqrt{H_0^{\perp} (H_0^{\perp} - 4\pi M_{\text{eff}}^{\perp})}, \quad (3)$$

where  $H_0^{\parallel}$  and  $H_0^{\perp}$  are the external field for in-plane and out-of-plane measurement, respectively.  $4\pi M_{\text{eff}}$  denotes the effective magnetization. The gyromagnetic ratio and effective magnetization are  $\gamma = 1.524$  MHz/Oe, and  $4\pi M_{\text{eff}} = 4,046$  kOe, respectively. We also conducted in-plane microwave measurements under applied electric fields, and describe the resonance as

$$f = \gamma \sqrt{(H_0^{\parallel} + \delta H_E) (H_0^{\parallel} + \delta H_E + 4\pi M_{\text{eff}}^{\parallel})}. \quad (4)$$

Since  $\delta H_E$  is positive and parallel to the external magnetic field, a resonance external field is reduced by the application of an applied electric field. This relationship is depicted in Fig. 3. A maximum  $E$ -field-induced magnetic field

TABLE I. Summary of magnetoelectric coupling parameters for some laminated structures. PZT—lead zirconate titanate; NFO—nickel ferrite; LFO—lithium ferrite; YIG—yttrium iron garnet ferrite; and GGG—gadolinium gallium garnet.

Structure	$A$ (Oe cm/kV)	$\delta H_E$ (Oe)	$\Delta f$ (MHz)	$E$ (kV/cm)	$f$ (GHz)	Ref.
YIG/PZT	0.39	7	40	18	5	16
YIG/PZT	0.88	8.75	25	10	2–10	12
NFO/PZT	1.1	330	925	300	9.3	17
LFO/PZT	0.39	117	...	300	9.3	17
LFO/PZT	0.5	40	...	80	9.3	11
YIG/GGG/PMN-PT	5.5	44	122	8	9.3	18
YIG/PMN-PT	5.0	150	420	30	9.3	11
FeGaB/Si/PMN-PT	3.4	28	900	8	2–3	6
Ni <sub>2</sub> MnGa/PMN-PT	41	230	370	6	9.5	Present

shift  $\delta H_E$  of 230 Oe is obtained for an  $E=6$  kV/cm. By Eq. (4), the corresponding maximum frequency shift  $\Delta f$  is calculated to be  $\sim 370$  MHz at  $E=6$  kV/cm. Importantly, Fig. 3 illustrates a clear linear relationship between both the magnetic field shift and resonance frequency shift brought about by the application of the electric field on the PMN-PT substrate. From the fitting results, the magnetoelectric constant  $A=41.3$  Oe cm/kV and the resonance frequency tunability  $66.5$  kHz cm/V are deduced.

Table I summarizes important results for different layered structures recently reported.<sup>6,11,12,16–18</sup> In review, we observe that the Heusler-based structure reported here demonstrates the largest reported magnetoelectric constant for ME heterostructures. Further, this *giant* magnetoelectric constant occurs under the application of comparatively modest electric fields of 0–6 kV/cm.

In summary, we report a giant magnetoelectric coupling in a Ni<sub>2</sub>MnGa/PMN-PT heterostructure; nearly eight times the previously reported ME coupling constant values for other ME layered structures. This results from the large magnetostrictive behavior of the Ni<sub>2</sub>MnGa Heusler alloy ribbon in combination with a PMN-PT piezoelectric crystal transducer. The composite structure exhibits an induced magnetic

field  $\sim 230$  Oe in response to a moderate electric field ( $\sim 6$  kV/cm) across the PMN-PT crystal. It is noteworthy that a few hundred Oersted of induced magnetic field may allow for the realization of  $E$ -field tunable microwave devices, such as, microwave resonators, filters, phase shifters,  $E$ -field tunable transducers, etc. These devices should be lighter and cost effective to fabricate and offer enhanced functionality compared with the state of technology.

This work was supported by the Office of Naval Research under Grant No. N00014-05-1-0349.

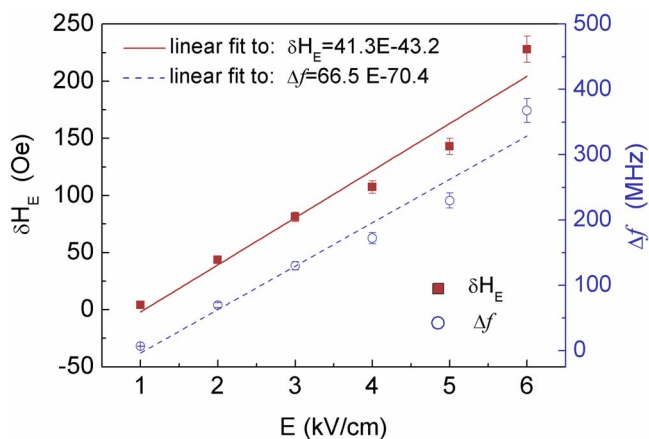


FIG. 3. (Color online) Electric field dependence of FMR frequency shift and induced internal magnetic field in a laminated Ni<sub>2</sub>MnGa/PMN-PT composite.

- <sup>1</sup>T. Kimura, *Annu. Rev. Mater. Res.* **37**, 387 (2007).
- <sup>2</sup>R. Ramesh and N. A. Spaldin, *Nat. Mater.* **6**, 21 (2007).
- <sup>3</sup>J. Zhai, Z. Xing, S. Dong, J. Li, and D. Viehland, *J. Am. Ceram. Soc.* **91**, 351 (2008).
- <sup>4</sup>M. I. Bichurin, D. Viehland, and G. Srinivasan, *J. Electroceram.* **19**, 243 (2007).
- <sup>5</sup>C. W. Nan, M. I. Bichurin, S. Dong, and D. Viehland, *J. Appl. Phys.* **103**, 031101 (2008).
- <sup>6</sup>J. Lou, D. Reed, C. Pettiford, M. Liu, P. Han, S. Dong, and N. X. Sun, *Appl. Phys. Lett.* **92**, 262502 (2008).
- <sup>7</sup>G. H. Wu, C. H. Yu, L. Q. Meng, J. L. Chen, F. M. Yang, S. R. Qi, W. S. Zhan, Z. Wang, Y. F. Zheng, and L. C. Zhao, *Appl. Phys. Lett.* **75**, 2990 (1999).
- <sup>8</sup>P. Han, W. Yan, J. Tian, X. Huang, and H. Pan, *Appl. Phys. Lett.* **86**, 052902 (2005).
- <sup>9</sup>M. I. Bichurin, I. A. Kornev, V. M. Petrov, A. S. Tatarenko, Yu. V. Kiliba, and G. Srinivasan, *Phys. Rev. B* **64**, 094409 (2001).
- <sup>10</sup>J. Worgull, E. Petti, and J. Trivisonno, *Phys. Rev. B* **54**, 15695 (1996).
- <sup>11</sup>A. S. Tatarenko, V. Gheevarghese, G. Srinivasan, O. V. Antonenkov, and M. I. Bichurin, "Microwave magnetoelectric effects in ferrite—piezoelectric composites and dual electric and magnetic field tunable filters," *J. Electroceram.* (to be published).
- <sup>12</sup>Y. K. Fetisov and G. Srinivasan, *Appl. Phys. Lett.* **88**, 143503 (2006).
- <sup>13</sup>G. Srinivasan, A. S. Tatarenko, and M. I. Bichurin, *Electron. Lett.* **41**, 596 (2005).
- <sup>14</sup>B. D. Shanina, A. A. Konchits, S. P. Kolesnik, V. G. Gavriljuk, I. N. Glavatskij, N. I. Glavatska, O. Söderberg, V. K. Lindroos, and J. Foct, *J. Magn. Magn. Mater.* **237**, 309 (2001).
- <sup>15</sup>C. Vittoria, *Microwave Properties of Magnetic Films* (World Scientific, Singapore, 1993).
- <sup>16</sup>Y. K. Fetisov and G. Srinivasan, *Appl. Phys. Lett.* **93**, 033508 (2008).
- <sup>17</sup>M. I. Bichurin, V. M. Petrov, and Yu. V. Kiliba, *Phys. Rev. B* **66**, 134404 (2002).
- <sup>18</sup>S. Shastry, G. Srinivasan, M. I. Bichurin, V. M. Petrov, and A. S. Tatarenko, *Phys. Rev. B* **70**, 064416 (2004).